Strong quantum effects in an almost classical antiferromagnet on a kagome lattice

A. L. Chernyshev
Department of Physics and Astronomy, University of California, Irvine, California 92697, USA
(Received 14 May 2015; revised manuscript received 13 August 2015; published 4 September 2015)

Two ubiquitous features of frustrated spin systems stand out: massive degeneracy of their ground states and flat, or dispersionless, excitation branches. In real materials, the former is frequently lifted by secondary interactions or quantum fluctuations, in favor of an ordered or spin-liquid state, but the latter often survive. We demonstrate that flat modes may precipitate remarkably strong quantum effects even in the systems that are otherwise written off as almost entirely classical. The resultant spectral features should be reminiscent of the quasiparticle breakdown in quantum systems, only here the effect is strongly amplified by the flatness of spin-excitation branches, leading to the damping that is not vanishingly small even at $S \gg 1$. We provide a theoretical analysis of the excitation spectrum of the $S = 5/2$ iron jarosite to illustrate our findings and to suggest further studies of this and other frustrated spin systems.

DOI: 10.1103/PhysRevB.92.094409 PACS number(s): 75.10.Jm, 75.30.Ds, 75.40.Gb, 75.50.Ee

I. INTRODUCTION

Ever since their inception in the 1950s [1,2], frustrated spin systems have been a source of new ideas for a wide variety of problems; unconventional superconductivity [3], order-by-disorder phenomena [4], and correlated spin-liquid states [5] are among them. In the core of this fertility is the near degeneracy between a vast number of spin configurations, originating from competing interactions that are favoring mutually exclusive ground states. In frustrated magnetic materials and their models this massive degeneracy is responsible for an extreme sensitivity to subtle symmetry-breaking effects [6,7], a strongly amplified role of subleading coupling terms [8], a hierarchy of emergent energy scales [9], and order-by-disorder effects by thermal [10] and quantum fluctuations [11–13].

Concomitant of the ground-state degeneracy is another hallmark feature of the frustrated spin systems: flat excitation branches at low energies [6,8,11,14–17]. They owe their origin to both the topological structure of the underlying lattices that facilitate frustration and the insufficient constraint on the manifold of spin configurations. A subclass of frustrated magnets that exhibits flat modes prominently is the kagome-lattice antiferromagnets [5,14,18–24]. Under the influence of subleading interactions, the majority of the known kagome-lattice antiferromagnets order magnetically with spins forming noncollinear structures [15,16,25–27] that are often reminiscent of the classical 120° motif on each triangle, Fig. 1(a). Such a pattern is also emblematic of the geometric frustration, manifesting a compromise reached by spins locally to partially satisfy their antiferromagnetic trends.

The following aspect of this picture is crucial. The noncollinearity of the ordered spin pattern implies strong nonlinear, anharmonic effects [28]. The role of such effects in the ground-state selection of frustrated systems has been recognized since the early days of the field [6,11,29] and, recently, an accurate, systematic treatment of the quantum order-by-disorder effect due to them has received significant attention [12,30].

On the other hand, their role in the excitation spectra of the kagome-lattice antiferromagnets has been hardly touched upon. In this work, we demonstrate that the nonlinear terms can be particularly important in the spectral properties of the flat-band frustrated magnets, leading to spectacularly strong quantum effects even in the systems that are assumed almost classical. The resultant spectral features bear a remarkable similarity to the quasiparticle breakdown signatures in quantum spin and Bose liquids, such as superfluid ^{4}He [31,32], which exhibit characteristic termination points and ranges of energies where single-particle excitations are not well defined and are dominated instead by broad continua.

It is usually assumed that such drastic effects can only occur in the systems that are inherently quantum in nature [28,31,32]. In our case, their origin is in the near resonance decay of the "normal," i.e., dispersive, modes into pairs of the flat-mode excitations facilitated by the nonlinear couplings. As such, the effect is strongly amplified by the density of states of the flat modes and is very significant even for large-spin systems that can otherwise appear as purely classical, resulting in the damping effect $\Gamma_{\mathbf{k}}/\varepsilon_{\mathbf{k}} \sim 1$. While in the following we give a detailed account of the spectral properties of a specific kagome-lattice antiferromagnet, $S = 5/2$ Fe jarosite, encouraging its further investigation by inelastic neutron scattering, the outlined scenario should be applicable to a wide variety of other flat-band frustrated spin systems [14,17,33].

The paper is organized as follows. In Sec. II we provide a general argument for the resonant-like decay to exist in the frustrated flat-band systems and lay out a qualitative expectation, which highlights an unusual phenomenon: decays remain significant even in the $S \to \infty$ limit. In Sec. III we provide our results for the decay-dominated spectral features in Fe jarosite. Section IV gives a brief summary. Technical details are relegated to the Appendix.

II. NONLINEAR COUPLING AND RESONANT-LIKE DECAYS

Because of the noncollinear structure of the ground-state spin configuration, the interacting spin excitations in the kagome-lattice antiferromagnets are described by

$$\hat{\mathcal{H}} = \sum_{\mathbf{k}\mu} \varepsilon_{\mu\mathbf{k}} b^\dagger_{\mu\mathbf{k}} b_{\mu\mathbf{k}} + \frac{1}{2} \sum_{\mathbf{p}+\mathbf{q}=\mathbf{k}} \Phi^{\nu\eta\mu}_{\mathbf{qp};\mathbf{k}} b^\dagger_{\nu\mathbf{q}} b^\dagger_{\eta\mathbf{p}} b_{\mu\mathbf{k}} + \text{H.c.}, \quad (1)$$

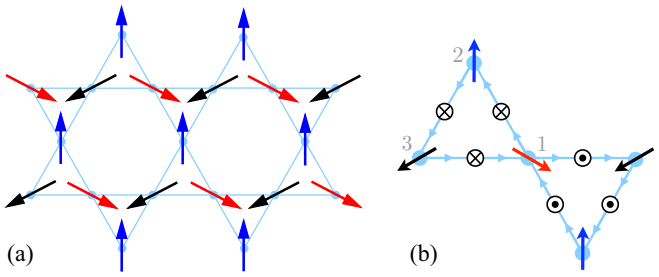

FIG. 1. (Color online) (a) $\mathbf{q}=0$ type of spin ordering on the kagome lattice. (b) Directions of the DM vectors. Arrows on the bonds show the ordering of $\mathbf{S}_i$ and $\mathbf{S}_j$ in (4).

where the first term accounts for the spin-wave energies while the second is an outcome of the anharmonic coupling of spins that results in the mutual transitions between excitation branches; see Appendix for details. Specifically, it couples dispersive excitations with the flat modes, allowing for the resonance-like decay of the former into the pairs of the latter. We note that this general form of bosonic Hamiltonian (1) occurs in a variety of contexts, including other frustrated antiferromagnets with noncollinear order [28,34], as well as spin liquids [35], valence-bond solids [36], and Bose liquids [31].

The full extent of the the $1/S$-expansion also involves quartic and source cubic terms; see Refs. [12,28]. Then, the magnon Green's function for the branch μ is

$$G^{-1}_{\mu\mathbf{k}}(\omega)=\omega-\varepsilon_{\mu\mathbf{k}}-\Sigma_{\mu\mathbf{k}}(\omega), \tag{2}$$

in which the self-energy $\Sigma_{\mu\mathbf{k}}(\omega)$ includes all such terms. However, it is only decay terms in (1) that are responsible for the resonance-like decay phenomenon discussed in this work. Given the off-resonance character of the source term, the Hartree-Fock nature of the quartic terms, and the large-S limit of the problem, one can safely approximate the self-energy by its on-shell imaginary part, i.e., by $\Sigma_{\mu\mathbf{k}}(\omega)|_{\omega=\varepsilon_{\mu\mathbf{k}}}\approx -i\Gamma_{\mu\mathbf{k}}$. The decay rate $\Gamma_{\mu\mathbf{k}}$ in the lowest-order approximation is given by

$$\Gamma_{\mu\mathbf{k}}=\frac{\pi}{2}\sum_{\mathbf{q},\nu\eta}\left|\Phi^{\nu\eta\mu}_{\mathbf{q},\mathbf{k}-\mathbf{q};\mathbf{k}}\right|^2\delta(\varepsilon_{\mu\mathbf{k}}-\varepsilon_{\nu\mathbf{q}}-\varepsilon_{\eta\mathbf{k}-\mathbf{q}}), \tag{3}$$

where the sum is over the branches of the decay products and an explicit form of the vertex $\Phi^{\nu\eta\mu}_{\mathbf{q},\mathbf{k}-\mathbf{q};\mathbf{k}}$ is given in the Appendix. With that, evaluation of the spectral function $A_{\mu\mathbf{k}}(\omega)=-(1/\pi)\mathrm{Im}G_{\mu\mathbf{k}}(\omega)$ is also straightforward.

The anharmonic cubic terms appear in the Hamiltonians of the noncollinear magnets via bosonization of the terms that have a form $\sim S^z_i S^{x(y)}_j$ in the local reference frame of the ordered moments [28]. Because of that, cubic vertices in (3) necessarily scale with the spin value as $\Phi^{\nu\eta\mu}_{\mathbf{q},\mathbf{p};\mathbf{k}}\propto\sqrt{S}$. Since the energies of the decay products scale as $\varepsilon_{\nu\mathbf{q}}\propto S$, it follows that $\Gamma_{\mu\mathbf{k}}$ in (3) must be spin-independent. Contributions to the decay rate from the higher-order terms should then follow a natural $1/S$ expansion with the exception of some special contours in $\mathbf{k}$ space where a $\log(S)$ enhancement in (3) is produced due to Van Hove singularities of the two-magnon continuum [28,34]. Therefore, one can conclude that for magnets with $S\gg 1$, damping of higher-energy magnetic excitations due to decays into lower-energy ones must be small compared to the excitation energy. In other words, generally, $\Gamma_{\mu\mathbf{k}}/\varepsilon_{\mu\mathbf{k}}\propto 1/S$ and thus one expects that effects of decays can be significant only for low-S, quantum magnets [28].

Here we offer a general scenario in which this seemingly invincible logic fails dramatically. If both decay products belong to the flat modes with constant energy ε_1, a remarkably stronger effect must be taking place. Namely, in this case the self-energy of the dispersive modes exhibits an essential singularity at the energy $2\varepsilon_1$, and, formally, the linewidth $\Gamma_{\mu\mathbf{k}}$ in (3) is infinite at this energy, the effect we refer to as the resonance-like decay.

In reality, quantum fluctuations of the same origin, i.e., coming from the anharmonic cubic terms, also generate effective further-neighbor J_2 spin couplings [11,12], which necessarily warp the flat mode and thus provide natural means of regularizing this essential singularity. However, the resultant fluctuation-induced bandwidth of the flat mode is now S-independent, $\delta\varepsilon_{\nu\mathbf{q}}\propto O(S^0)$, so that the regularized resonance-like broadening in the vicinity of $2\varepsilon_1$ must scale together with the excitation energy: $\Gamma_{\mu\mathbf{k}}\propto\varepsilon_{\mu\mathbf{k}}\propto S$. This qualitative consideration implies a spectacular quantum effect: a very strong damping, eliminating spectral weight from the respective energy range even in large-S magnets. Thus, frustration provides necessary and sufficient ingredients for the proliferation of the intrinsically quantum phenomenon of decays into inherently classical spin systems.

Altogether, we predict that anomalous broadening and a wipe-out of the spectral weight, associated with the resonant-like decays, should be common in the spectra of the flat-band frustrated systems. In practice, we argue that the quasiparticle breakdown with characteristic termination points and ranges of energies dominated by broad continua must be present in the $S=5/2$ kagome lattice Fe jarosite.

III. Fe JAROSITE

In realistic kagome-lattice antiferromagnets, the degeneracy within the manifold of classical 120° states is, most commonly, lifted by the symmetry-breaking Dzyaloshinskii-Moriya (DM) terms [25,26,37], yielding the Hamiltonian that closely describes Fe jarosite [15,16] and other systems [27,38,39]:

$$\hat{\mathcal{H}}=\sum_{\langle ij\rangle}(J\mathbf{S}_i\cdot\mathbf{S}_j+\mathbf{D}\cdot\mathbf{S}_i\times\mathbf{S}_j), \tag{4}$$

where summation is over the nearest-neighbor bonds and $\mathbf{D}=(0,0,\mp D_z)$ on the up/down triangles with the order of the site indices in (4) shown in Fig. 1(b). The out-of-plane DM interaction lifts the degeneracy and selects the $\mathbf{q}=0$ ground state, i.e., a "ferro" 120° pattern, Fig. 1(a). A small in-plane DM term [16] is neglected for simplicity.

Given the large spin value, $S=5/2$, we estimate that the ordered moment should be nearly 90% of its classical value [40]. Similarly, the results of the earlier neutron scattering in Fe jarosite [15] have been interpreted as fully describable by the linear spin-wave theory [16], a construction whose validity we question next.

Our Fig. 2(a) shows the linear spin-wave theory fits of the neutron-scattering data [15] using model (4) where three

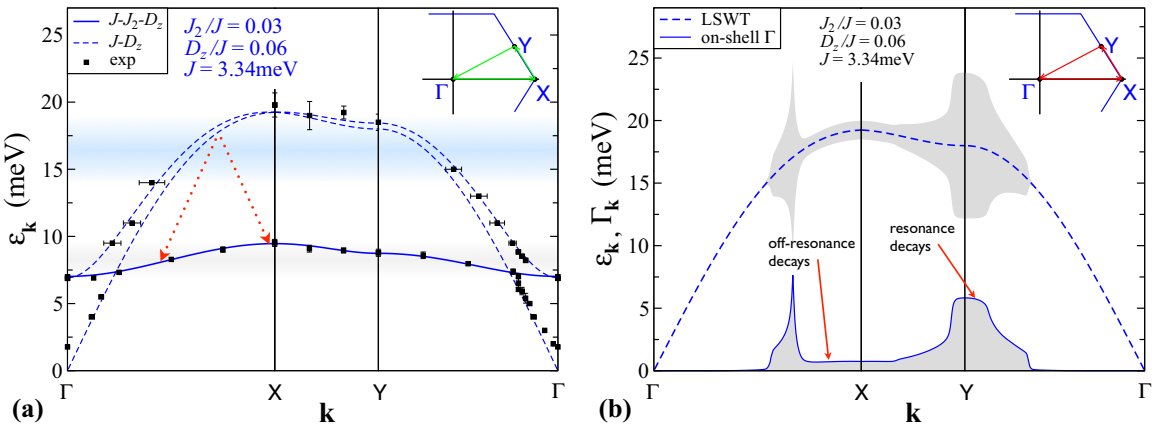

FIG. 2. (Color online) (a) Neutron-scattering data from [15] along the $\Gamma XY\Gamma$ path (inset). Lines are linear spin-wave theory fits of the dispersive modes (dashed) using (4), and the flat mode (solid) with J_2 added to (4), parameters are as shown. Lower shaded area highlights the flat band, upper is the set of energies of two flat modes. Arrows imply a decay process into two flat modes. (b) Lower curve with the shading is the on-shell $\Gamma_{\mathbf{k}}$ from (3). Dashed line is the linear spin-wave theory energy of the gapless dispersive mode from (a), shaded area shows the half-width boundaries of a Lorentzian peak, $\varepsilon_{\mathbf{k}} \pm \Gamma_{\mathbf{k}}$.

distinct excitations branches are easy to identify. The DM anisotropy shifts the flat mode from zero energy to $\varepsilon_{1\mathbf{k}} \approx JS\sqrt{6d_M}$, where $d_M = \sqrt{3}D_z/J$; see Appendix A. The flat mode is also not entirely flat. This was interpreted [16] as a sign of a phenomenological next-nearest-neighbor superexchange J_2, ignoring its possible quantum origin [11,12]. Since in the following we do not attempt a fully self-consistent calculation, the same interpretation suffices, with an explicit expression for the dispersive flat mode given in the Appendix. Aside from this slight dichotomy with the origin of the flat-mode dispersion, the linear spin-wave theory seems to provide a spectacular account of the data without the need of any quantum effects.

However, we point out that the spectral weight is conspicuously missing from experimental data in the range of energies 15–19 meV in Fig. 2(a); i.e., no signal has been detected there. While this feature has not been emphasized in Ref. [15] and one may argue that the collected experimental data points were simply too sparse, the missing band is strongly implied by our discussion, as it is exactly in the range of twice the energy of the flat mode, $2\varepsilon_{1\mathbf{k}}$; see Fig. 2(a).

In Fig. 2(b) we present the results of the on-shell calculation of $\Gamma_{\mathbf{k}}$ for the gapless dispersive mode using (3) with the flat-mode dispersion induced by J_2 for the same parameters as in Fig. 2(a); see the Appendix for details. As we discuss later, the dynamical structure factor allows us to view modes selectively in different parts of the $\mathbf{k}$ space and in different polarizations [40]. The results for the damping are combined with the energy $\varepsilon_{\mathbf{k}}$ of the mode with the shaded area representing half-width boundaries of a Lorentzian peak, $\varepsilon_{\mathbf{k}} \pm \Gamma_{\mathbf{k}}$. We have also verified [40] that the effect of renormalization on the real part of the spectrum is minor, in agreement with approximation in (3).

Our Fig. 2(b) demonstrates that the spin-wave excitation is well defined until a sharp threshold at about $2\varepsilon^{\min}_{1\mathbf{k}}$. Above that energy, the broadening reaches about one-third of the bandwidth signifying an overdamped spectrum, consistent with the missing spectral weight in the experimental data. The sharp transition implies a threshold singularity and other spectral features that are characteristic to the quasiparticle breakdown phenomenon in quantum Bose liquids and $S = 1/2$ spin liquids [31,32]. There is a partial reconstruction of the spectrum at the energies above $2\varepsilon^{\max}_{1\mathbf{k}}$ where decays are no more resonant-like as indicated in the figure, i.e., occurring due to other, nonresonant channels, but still providing a sizable broadening to the spectrum.

The nonresonant decays result in a typical broadening $\Gamma \sim 0.25J$, in accord with similar results for the triangular lattice [34,41] and other frustrated spin systems [28]. By contrast, the broadening in the resonant-decay region in Fig. 2(b) reaches $\Gamma \approx 1.7J$, an effect larger by a factor exceeding $2S$ for the considered $S = 5/2$ model of Fe jarosite. This is in a remarkable agreement with our qualitative discussion on the scaling of the resonance-like decay rate with S, provided after Eq. (3) above.

We note that the broadening on the top of the band in the nonresonant region translates to less than 1 meV, below the experimental resolution of Ref. [15] in which all the data were described as resolution limited. The current resolution of the neutron-scattering experiments is easily an order of magnitude higher. We also point out that our consideration is aimed at the strong qualitative features of the spectrum of a representative flat-band frustrated spin system, not on the minor quantitative details. As such, small discrepancies with some of the data may occur due to, e.g., neglect of the in-plane DM terms, but should be considered as secondary.

Dynamical structure factor

To demonstrate the effect of decays, we performed a calculation of the magnon spectral functions, $A_{\nu\mathbf{q}}(\omega)$, quantities directly related to the spin-spin dynamical correlation function via

$$\mathcal{S}^{\alpha\alpha}(\mathbf{q},\omega) \propto \int dt\, e^{i\omega t}\left\langle S^{\alpha}_{\mathbf{q}}(t)S^{\alpha}_{-\mathbf{q}}\right\rangle \propto \sum_{\nu} F^{\alpha}_{\nu\mathbf{q}} A_{\nu\mathbf{q}}(\omega). \quad (5)$$

Here, the kinematic form factors $F^{\alpha}_{\nu\mathbf{q}}$ allow us to "filter out" spectral contributions of some of the modes to the in-plane and the out-of plane components of $\mathcal{S}(\mathbf{q},\omega)$ in the portions of the $\mathbf{q}$ space while highlighting the other ones: a phenomenon

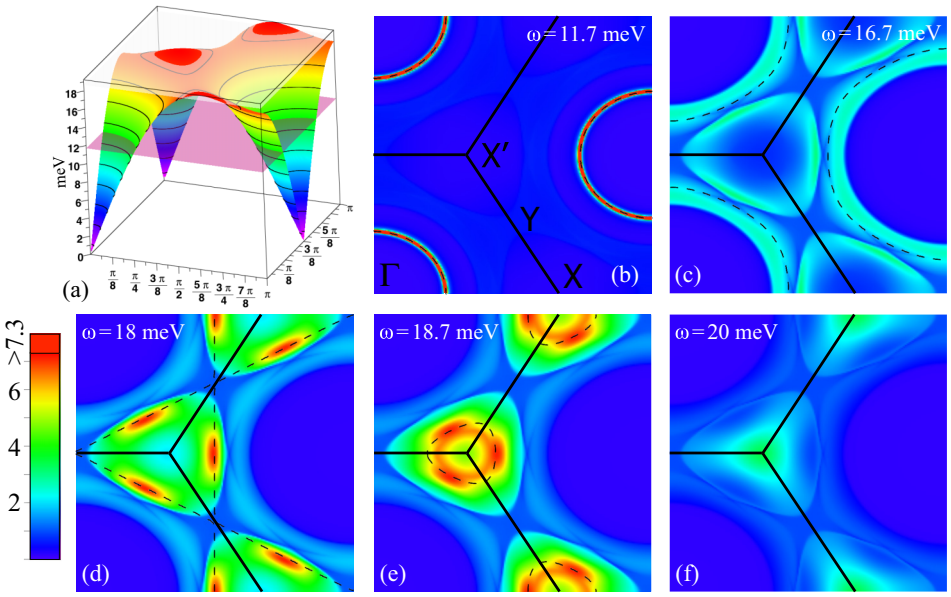

FIG. 3. (Color online) (a) A 3D plot of the magnon dispersion for Fe jarosite within the linear spin-wave theory with planes of the cuts in (b) and (e). (b)–(f) Intensity maps of $A_{\mathbf{q}}(\omega)$ in units of $(2SJ)^{-1}$ vs $\mathbf{q}$ throughout the Brillouin zone for a set of energies. Intensity scale is as described in text. Dashed black lines are peak positions from the linear spin-wave theory.

akin to the extinction of the Bragg peaks in the non-Bravias lattices [40]. Using this feature, we concentrate only on one of the dispersive modes.

A dramatic view on the drastic transformations of the spectrum can be observed in constant-energy cuts of the dynamical structure factor in the range of energies affected by the resonance-like decays. In Fig. 3, we present intensity maps of such constant-energy cuts for $A_{\nu\mathbf{q}}(\omega)$, a close proxy of the dynamical structure factor $\mathcal{S}(\mathbf{q},\omega)$, for the dispersive magnon mode for the energies ranging from 11.7 meV to 20 meV. The upper cutoff of the spectral function is chosen to correspond to the maximal height of the peaks in the nonresonant decay region in Fig. 2(b) and translates into the broadening $\Gamma_{\mathbf{k}} \approx 0.73$ meV for the Fe-jarosite values of S and J, which should be resolvable by the modern neutron-scattering measurements.

The first of the cuts is below the threshold energy $2\varepsilon^{\min}_{1\mathbf{k}}$ and shows a very close accord of the sharp intensity peaks in $A_{\nu\mathbf{q}}(\omega)$ with the expectations from the linear, noninteracting spin-wave theory, shown by the dashed lines. The three subsequent cuts, Figs. 3(c)–3(e), are from within the resonant-decay band, $2\varepsilon^{\min}_{1\mathbf{k}} < \omega < 2\varepsilon^{\max}_{1\mathbf{k}}$, where one can observe strong deviation from such expectations, massive redistribution of the spectral weight into different regions of the $\mathbf{q}$ space, and a multitude of intriguing "shadow" features, reflecting Van Hove singularities in the two-particle density of states of the decay products [41]. The last cut, Fig. 3(f), is nominally above the top of the magnon band and should be expected to show zero intensity everywhere. Instead, it is also affected by the spectral weight redistribution and retains some of the features of the other cuts. Altogether, Fig. 2(b) and Fig. 3 offer a comprehensive theoretical insight into the nontrivial features of the dynamical structure factor of a flat-band kagome-lattice antiferromagnet, which originate from the decays of magnetic excitations facilitated by the nonlinear couplings.

IV. SUMMARY

To summarize, we have outlined a general scenario for drastic transformations in the spectra of frustrated magnets that feature flat modes and have substantiated it by a consideration of the spin-spin structure factor of the large-S kagome-lattice system Fe jarosite. Our study calls for further studies in these systems.

We would also like to comment that recently, the broad features in the spectra of magnetic systems have become a direct sign of fractionalized excitations of prospective spin-liquid phases [42–45]. In this work, we have provided a case study of an excitation spectrum of a strongly frustrated but almost classical and well-ordered kagome-lattice antiferromagnet, for which we have demonstrated extremely strong broadening and even a complete and spectacular wipe-out of a part of its spectrum. Here, the broad features are due to flat or weakly dispersive modes, a hallmark feature of a variety of frustrated spin systems, and due to a noncollinearity of spins in the ground state, again an outcome of competing interactions. Thus, this is also a cautionary tale, because the same reasons that may lead to the spin-liquid behavior may also favor strong coupling and decays among quasiparticles.

ACKNOWLEDGMENTS

We acknowledge numerous enlightening discussions with Michael Zhitomirsky and a useful conversation with Collin Broholm. We are thankful to Kittiwit Matan for sharing his previously published data. This work was supported by the US Department of Energy, Office of Science, Basic Energy Sciences, under Award No. DE-FG02-04ER46174. We would like to thank Aspen Center for Physics, where part of this work was done, for hospitality. The work at Aspen was supported in part by NSF Grant No. PHYS-1066293.

APPENDIX: TECHNICAL DETAILS

1. Spin-wave theory

Following the approach outlined in Refs. [8,12], one can diagonalize the harmonic part of the Hamiltonian in (4) to

obtain the spin-wave energies

$$\varepsilon_{1\mathbf{k}} = 2JS\sqrt{3d_M(1+d_M)/2}, \tag{A1}$$

for the "flat mode," and

$$\varepsilon_{2(3)\mathbf{k}} = 2JS\sqrt{1+d_M}\sqrt{1+d_M-\gamma_{\mathbf{k}}-d_M(1\pm\sqrt{1+8\gamma_{\mathbf{k}}})/4}, \tag{A2}$$

for the dispersive modes, $d_M=\sqrt{3}D_z/J$ here.

Corrections due to effective J_2 interactions can be taken into account perturbatively to yield [40] the dispersion of the "flat mode,"

$$\varepsilon_{1\mathbf{k}} = 2JS\sqrt{3(1+d_M)/2 + j_2\big(1-\lambda^{(1)}_{1,\mathbf{k}}/2\big)} \times\sqrt{d_M + j_2\big(1+\lambda^{(1)}_{1,\mathbf{k}}\big)} + O\big(j_2^2\big), \tag{A3}$$

where $j_2 = J_2/J$ and

$$\begin{aligned} \lambda^{(1)}_{1,\mathbf{k}} &= [f_2(\mathbf{k}) - f_1(\mathbf{k})]/(1-\gamma_{\mathbf{k}}), \\ \text{with}\quad f_1(\mathbf{k}) &= c_1'c_1 + c_2'c_2 + c_3'c_3, \\ f_2(\mathbf{k}) &= c_1'c_2c_3 + c_2'c_1c_3 + c_3'c_1c_2, \end{aligned} \tag{A4}$$

with the shorthand notations $c_n=\cos(q_n)$, $c_1'=\cos(q_3+q_2)$, $c_2'=\cos(q_3-q_1)$, $c_3'=\cos(q_1+q_2)$, where $q_n=\mathbf{k}\cdot\boldsymbol{\delta}_n/2$, and $\boldsymbol{\delta}_n$ are the primitive vectors of the kagome lattice.

The diagonalization of the harmonic part of (4) implies a two-step procedure [8,12] with the unitary transformation of the original Holstein-Primakoff bosons

$$a_{\alpha\mathbf{k}} = \sum_{\nu} w_{\nu,\alpha}(\mathbf{k})\, d_{\nu\mathbf{k}}, \tag{A5}$$

followed by the usual Bogolyubov transformation for each of the individual species of d boson; see Ref. [12] for details and for the explicit form of the eigenvectors $\mathbf{w}_\nu = (w_{\nu,1}(\mathbf{k}), w_{\nu,2}(\mathbf{k}), w_{\nu,3}(\mathbf{k}))$.

2. Cubic terms

Due to noncollinear 120° spin structure, cubic anharmonic coupling of the spin waves occurs [12,28]. It originates from the $S_i^x S_j^z$ terms in (4), written in the local reference frame [12]. In the bosonic representation they yield

$$\hat{\mathcal{H}}_3 = J(1+d_M/3)\sqrt{\frac{S}{2}}\sum_{i,j}\sin\theta_{ij}(a_i^\dagger a_j^\dagger a_j + \text{H.c.}), \tag{A6}$$

where $\theta_{ij}=\pm 120^\circ$ is the angle between two neighboring spins.

Assuming the spins in the $\mathbf{q}=0$ state, Fig. 1(a), and using the unitary and Bogolyubov transformations mentioned above gives the "source," $b^\dagger b^\dagger b^\dagger$, and the "decay," $b^\dagger b^\dagger b$, terms; see Ref. [12] where the effects of the former were discussed. The decay part of the Hamiltonian is

$$\hat{\mathcal{H}}_3 = \frac{1}{2!}\frac{1}{\sqrt{N}}\sum_{\mathbf{k}+\mathbf{q}=\mathbf{p}} \Phi^{\nu\mu\eta}_{\mathbf{qk};\mathbf{p}}\, b^\dagger_{\nu\mathbf{q}} b^\dagger_{\mu\mathbf{k}} b_{\eta\mathbf{p}} + \text{H.c.}, \tag{A7}$$

with the vertex

$$\Phi^{\nu\mu\eta}_{\mathbf{qk};\mathbf{p}} = -J\sqrt{\frac{3S}{2}}\,\widetilde{\Phi}^{\nu\mu\eta}_{\mathbf{qk};\mathbf{p}}, \tag{A8}$$

which is explicitly $\propto\sqrt{S}$. The symmetrized dimensionless vertex $\widetilde{\Phi}^{\nu\mu\eta}_{\mathbf{qk};\mathbf{p}}$ is given by

$$\begin{aligned} \widetilde{\Phi}^{\nu\mu\eta}_{\mathbf{qk};\mathbf{p}} &= F^{\nu\mu\eta}_{\mathbf{qk};\mathbf{p}}(u_{\nu\mathbf{q}}+v_{\nu\mathbf{q}})(u_{\mu\mathbf{k}}u_{\eta\mathbf{p}}+v_{\mu\mathbf{k}}v_{\eta\mathbf{p}}) \\ &+ F^{\mu\eta\nu}_{\mathbf{kpq}}(u_{\mu\mathbf{k}}+v_{\mu\mathbf{k}})(u_{\nu\mathbf{p}}u_{\eta\mathbf{q}}+v_{\nu\mathbf{p}}v_{\eta\mathbf{q}}) \\ &+ F^{\eta\nu\mu}_{\mathbf{pqk}}(u_{\eta\mathbf{p}}+v_{\eta\mathbf{p}})(u_{\nu\mathbf{q}}v_{\mu\mathbf{k}}+v_{\nu\mathbf{q}}u_{\mu\mathbf{k}}), \end{aligned} \tag{A9}$$

where $u_{\nu\mathbf{k}}$ and $v_{\nu\mathbf{k}}$ are the Bogolyubov parameters and the amplitudes $F^{\nu\mu\eta}_{\mathbf{qkp}}$ are given by

$$F^{\nu\mu\eta}_{\mathbf{qkp}} = \sum_{\alpha\beta}\epsilon^{\alpha\beta\gamma}\cos(q_{\beta\alpha})\, w_{\nu,\alpha}(\mathbf{q})w_{\mu,\beta}(\mathbf{k})w_{\eta,\beta}(\mathbf{p}), \tag{A10}$$

where $\epsilon^{\alpha\beta\gamma}$ is the Levi-Civita antisymmetric tensor, and shorthand notations are $q_{\beta\alpha}=\mathbf{q}\boldsymbol{\rho}_{\beta\alpha}$ and $\boldsymbol{\rho}_{\beta\alpha}=\boldsymbol{\rho}_\beta-\boldsymbol{\rho}_\alpha$; here $\boldsymbol{\rho}_\alpha$ are the atom's positions within the unit cell.

3. Self-energy, spectral function, and structure factor

Using the standard diagrammatic rules for (1), we obtain the second-order decay self-energy

$$\Sigma_{\mu\mathbf{k}}(\omega) = \frac{1}{2}\sum_{\mathbf{q},\nu\eta}\frac{\big|\Phi^{\nu\eta\mu}_{\mathbf{q},\mathbf{k}-\mathbf{q};\mathbf{k}}\big|^2}{\omega-\varepsilon_{\nu\mathbf{q}}-\varepsilon_{\eta\mathbf{k}-\mathbf{q}}+i\delta}, \tag{A11}$$

which contributes to the $1/S$ correction to the magnon energy. The magnon Green's function for the branch μ is given by (2). Since only the decay terms are responsible for the resonance-like decay phenomena, one can approximate the self-energy by its on-shell imaginary part; i.e.,

$$\Sigma_{\mu\mathbf{k}}(\omega) \approx i\,\mathrm{Im}\Sigma_{\mu\mathbf{k}}(\varepsilon_{\mu\mathbf{k}}) = -i\,\Gamma_{\mu\mathbf{k}}, \tag{A12}$$

which is given by (3). Clearly, the dispersion of the flat mode in (A3) is crucial for the decays into two of them, as otherwise this channel would produce essential singularity in (A11) and in $\Gamma_{\mu\mathbf{k}}$. With that, evaluation of the spectral function $A_{\mu\mathbf{k}}(\omega) = -(1/\pi)\mathrm{Im}G_{\mu\mathbf{k}}(\omega)$ can be performed numerically.

The diagonal components of the dynamical structure factor, or the spin-spin dynamical correlation function, which contribute directly to the inelastic neutron-scattering cross section, are given by

$$\mathcal{S}^{\alpha_0\alpha_0}(\mathbf{q},\omega) = \int_{-\infty}^{\infty}\frac{dt}{2\pi}\, e^{i\omega t}\big\langle S^{\alpha_0}_{\mathbf{q}}(t)S^{\alpha_0}_{-\mathbf{q}}\big\rangle, \tag{A13}$$

where α_0 refers to the laboratory frame $\{x_0,y_0,z_0\}$. Given the coplanar spin configuration, it is convenient to separate the in-plane and out-of-plane components of $\mathcal{S}^{\mathrm{tot}}(\mathbf{q},\omega)$. Assuming equal contribution of all three α_0 components to the cross section, using the spin-wave mapping of spins on bosons with the two-step transformation described above, after some algebra, one can obtain the leading contributions to the structure factor as directly related to the spectral function

$$\mathcal{S}^{\mathrm{in(out)}}(\mathbf{q},\omega) = \sum_{\nu} F^{\mathrm{in(out)}}_{\nu\mathbf{q}} A_{\nu\mathbf{q}}(\omega), \tag{A14}$$

where $F^{\mathrm{in(out)}}_{\nu\mathbf{q}}$ are the kinematic form factors. It is important to note that the kinematic form factors are modulated in the $\mathbf{q}$ space and are suppressed in one of the Brillouin zones while they are maximal in the others [40]. This effect is characteristic to the non-Bravias lattices and is similar

to the effect of extinction of some of the Bragg peaks in them. Because of that, one may be able to highlight spectral contribution of one of the magnon branches while "filtering out" the others by selecting a particular component of the structure factor in a particular Brillouin zone. Our analysis demonstrates that the out-of plane component of $\mathcal{S}(\mathbf{q},\omega)$ should be totally dominated by only one of the dispersive modes (gapless) in one of the three distinct Brillouin zones. This feature can be useful for future neutron-scattering experiments.

[1] G. H. Wannier, Phys. Rev. **79**, 357 (1950).
[2] A. Yoshimori, J. Phys. Soc. Jpn. **14**, 807 (1959).
[3] P. W. Anderson, Science **235**, 1196 (1987).
[4] J. Villain, R. Bidaux, J.-P. Carton, and R. Conte, J. Phys. (Paris) **41**, 1263 (1980).
[5] L. Balents, Nature (London) **464**, 199 (2010).
[6] J. T. Chalker, P. C. W. Holdsworth, and E. F. Shender, Phys. Rev. Lett. **68**, 855 (1992).
[7] D. A. Huse and A. D. Rutenberg, Phys. Rev. B **45**, 7536 (1992).
[8] A. B. Harris, C. Kallin, and A. J. Berlinsky, Phys. Rev. B **45**, 2899 (1992).
[9] M. Taillefumier, J. Robert, C. L. Henley, R. Moessner, and B. Canals, Phys. Rev. B **90**, 064419 (2014).
[10] J. N. Reimers and A. J. Berlinsky, Phys. Rev. B **48**, 9539 (1993).
[11] A. Chubukov, Phys. Rev. Lett. **69**, 832 (1992).
[12] A. L. Chernyshev and M. E. Zhitomirsky, Phys. Rev. Lett. **113**, 237202 (2014).
[13] G. Jackeli and A. Avella, arXiv:1504.01435.
[14] K. Matan, Y. Nambu, Y. Zhao, T. J. Sato, Y. Fukumoto, T. Ono, H. Tanaka, C. Broholm, A. Podlesnyak, and G. Ehlers, Phys. Rev. B **89**, 024414 (2014).
[15] K. Matan, D. Grohol, D. G. Nocera, T. Yildirim, A. B. Harris, S. H. Lee, S. E. Nagler, and Y. S. Lee, Phys. Rev. Lett. **96**, 247201 (2006).
[16] T. Yildirim and A. B. Harris, Phys. Rev. B **73**, 214446 (2006).
[17] N. d'Ambrumenil, O. A. Petrenko, H. Mutka, and P. P. Deen, Phys. Rev. Lett. **114**, 227203 (2015).
[18] J. S. Helton, K. Matan, M. P. Shores, E. A. Nytko, B. M. Bartlett, Y. Yoshida, Y. Takano, A. Suslov, Y. Qiu, J.-H. Chung, D. G. Nocera, and Y. S. Lee, Phys. Rev. Lett. **98**, 107204 (2007).
[19] T.-H. Han, J. S. Helton, S. Chu, D. G. Nocera, J. A. Rodriguez-Rivera, C. Broholm, and Y. S. Lee, Nature (London) **492**, 406 (2012).
[20] K. Matan, T. Ono, Y. Fukumoto, T. J. Sato, J. Yamaura, M. Yano, K. Morita, and H. Tanaka, Nat. Phys. **6**, 865 (2010).
[21] S. Yan, D. A. Huse, and S. R. White, Science **332**, 1173 (2011).
[22] M. Mambrini and F. Mila, Eur. Phys. J. B **17**, 651 (2000).
[23] Y. Iqbal, F. Becca, S. Sorella, and D. Poilblanc, Phys. Rev. B **87**, 060405 (2013).
[24] I. Rousochatzakis, Y. Wan, O. Tchernyshyov, and F. Mila, Phys. Rev. B **90**, 100406 (2014).
[25] M. Elhajal, B. Canals, and C. Lacroix, Phys. Rev. B **66**, 014422 (2002).
[26] A. Zorko, F. Bert, A. Ozarowski, J. van Tol, D. Boldrin, A. S. Wills, and P. Mendels, Phys. Rev. B **88**, 144419 (2013).
[27] H. Yoshida, Y. Michiue, E. Takayama-Muromachi, and M. Isobe, J. Mater. Chem. **22**, 18793 (2012).
[28] M. E. Zhitomirsky and A. L. Chernyshev, Rev. Mod. Phys. **85**, 219 (2013).
[29] J. von Delft and C. L. Henley, Phys. Rev. B **48**, 965 (1993).
[30] O. Götze and J. Richter, Phys. Rev. B **91**, 104402 (2015).
[31] M. B. Stone, I. A. Zaliznyak, T. Hong, C. L. Broholm, and D. H. Reich, Nature (London) **440**, 187 (2006).
[32] T. Masuda, A. Zheludev, H. Manaka, L.-P. Regnault, J.-H. Chung, and Y. Qiu, Phys. Rev. Lett. **96**, 047210 (2006).
[33] C. Wu, D. Bergman, L. Balents, and S. Das Sarma, Phys. Rev. Lett. **99**, 070401 (2007).
[34] A. L. Chernyshev and M. E. Zhitomirsky, Phys. Rev. Lett. **97**, 207202 (2006).
[35] M. E. Zhitomirsky, Phys. Rev. B **73**, 100404 (2006).
[36] L. Fritz, R. L. Doretto, S. Wessel, S. Wenzel, S. Burdin, and M. Vojta, Phys. Rev. B **83**, 174416 (2011).
[37] O. Cépas, C. M. Fong, P. W. Leung, and C. Lhuillier, Phys. Rev. B **78**, 140405 (2008).
[38] A. Zorko, S. Nellutla, J. van Tol, L. C. Brunel, F. Bert, F. Duc, J.-C. Trombe, M. A. de Vries, A. Harrison, and P. Mendels, Phys. Rev. Lett. **101**, 026405 (2008).
[39] I. Rousochatzakis, J. Richter, R. Zinke, and A. A. Tsirlin, Phys. Rev. B **91**, 024416 (2015).
[40] A. L. Chernyshev and M. E. Zhitomirsky, arXiv:1508.06632.
[41] A. L. Chernyshev and M. E. Zhitomirsky, Phys. Rev. B **79**, 144416 (2009).
[42] B. Dalla Piazza, M. Mourigal, N. B. Christensen, G. J. Nilsen, P. Tregenna-Piggott, T. G. Perring, M. Enderle, D. F. McMorrow, D. A. Ivanov, and H. M. Rønnow, Nat. Phys. **11**, 62 (2015).
[43] H. D. Zhou, C. Xu, A. M. Hallas, H. J. Silverstein, C. R. Wiebe, I. Umegaki, J. Q. Yan, T. P. Murphy, J.-H. Park, Y. Qiu, J. R. D. Copley, J. S. Gardner, and Y. Takano, Phys. Rev. Lett. **109**, 267206 (2012).
[44] H. D. Zhou, E. S. Choi, G. Li, L. Balicas, C. R. Wiebe, Y. Qiu, J. R. D. Copley, and J. S. Gardner, Phys. Rev. Lett. **106**, 147204 (2011).
[45] R. Coldea, D. A. Tennant, A. M. Tsvelik, and Z. Tylczynski, Phys. Rev. Lett. **86**, 1335 (2001).